

Disentangling the drivers of invasion spread in a vector-borne tree disease

Yutaka Osada¹  | Takehisa Yamakita²  | Etsuko Shoda-Kagaya³  |
Andrew M. Liebhold⁴  | Takehiko Yamanaka⁵ 

¹Graduate School of Life Sciences, Tohoku University, Miyagi, Japan

²R&D Center for Submarine Resources, Japan Agency for Marine-Earth Science and Technology, Yokohama, Japan

³Department of Forest Entomology, Forestry and Forest Products Research Institute, Forest Research and Management Organization, Tsukuba, Japan

⁴US Forest Service Northern Research Station, Morgantown, West Virginia

⁵Statistical Modeling Unit, Institute for Agro-Environmental Sciences, NARO, Tsukuba, Japan

Correspondence

Takehiko Yamanaka
Email: apple@affrc.go.jp

Funding information

JSPS Fellowship For Research In Japan (Short Term), Grant/Award Number: S10090

Handling Editor: Dylan Childs

Abstract

1. Pine wilt disease (PWD) invaded southern Japan in the early 1900s and has gradually expanded its range to northern Honshu (Japanese mainland). The disease is caused by a pathogenic North American nematode, which is transmitted by native pine sawyer beetles. Recently, the disease has invaded other portions of East Asia and Europe where extensive mortality of host pines is anticipated to resemble historical patterns seen in Japan.
2. There is a critical need to identify the main drivers of PWD invasion spread so as to predict the future spread and evaluate containment strategies in newly invaded world regions. But the coupling of pathogen and vector population dynamics introduces considerable complexity that is important for understanding this and other plant disease invasions.
3. In this study, we analysed historical (1980–2011) records of PWD infection and vector abundance, which were spatially extensive but recorded at coarse categorical levels (none, low and high) across 403 municipalities in northern Honshu. We employed a multistate occupancy model that accounted both for demographic stochasticity and observation errors in categorical data.
4. Analysis revealed that sparse sawyer populations had lower probabilities of transition to high abundance than did more abundant populations even when regional abundance stayed the same, suggesting the existence of positive density dependence, that is an Allee effect, in sawyer dynamics. Climatic conditions (average accumulated degree days) substantially limited invasion spread in northern regions, but this climatic influence on sawyer dynamics was generally weaker than the Allee effect.
5. Our results suggest that tactics (eg sanitation logging of infected pines) which strengthen Allee effects in sawyer dynamics may be effective strategies for slowing the spread of PWD.

KEYWORDS

Allee effect, Bayesian MCMC, multistate occupancy model, pine sawyer *Monochamus alternatus*, pine wilt disease (PWD), pine wood nematode *Bursaphelenchus xylophilus*, state-space modelling

This is an open access article under the terms of the Creative Commons Attribution License, which permits use, distribution and reproduction in any medium, provided the original work is properly cited.

© 2018 The Authors. *Journal of Animal Ecology* published by John Wiley & Sons Ltd on behalf of British Ecological Society

1 | INTRODUCTION

Following initial transport and establishment, invading populations proceed to expand their ranges into suitable habitat. This spread phase of biological invasions is driven by the coupling of population growth with dispersal; understanding and predicting the spread of invading species has considerable applied and theoretical significance (Hastings et al., 2005; Tisseuil et al., 2016). Many plant pathogens are vectored by insects, and the reliance of pathogens on vectors means that vector population dynamics play a key role in disease spread. The coupling of pathogen and vector population dynamics introduces considerable complexity that is important for understanding plant disease invasions (Nakazawa, Yamanaka, & Urano, 2012; Stout, Thaler, & Thomma, 2006).

One such insect-vectored invasive disease, pine wilt disease (PWD), is one of the most serious tree diseases in the world. It invaded Japan in the early 20th century where it proceeded to kill millions of trees (Mamiya, 1988; Togashi & Shigesada, 2006), but more recently, the disease has invaded other portions of East Asia (Kawai et al., 2006; Shin, 2008; Zhao, 2008) and Europe (Mota, Futai, & Vieira, 2009; Robinet, Opstal, Baker, & Roques, 2011) where it is feared likely to spread and cause comparable damage (Evans, McNamara, Braasch, Chadoeuf, & Magnusson, 1996). The disease is caused by an invasive pathogenic nematode, *Bursaphelenchus xylophilus* (Nematoda: Parasitaphelenchidae), native throughout

North America. In both its native and invaded ranges, the nematode is transmitted by endemic pine sawyer beetles, *Monochamus* spp. (Coleoptera: Cerambycidae). In Japan, the endemic vector is *Monochamus alternatus*.

To date, PWD has spread through pine forests in the Japanese islands of Kyushu, Shikoku and Honshu (Togashi & Shigesada, 2006). Currently, Tohoku, the northern region of Honshu, contains the active invasion frontier of PWD in mainland Japan (Figure 1). PWD has steadily expanded its range through Honshu northward, but its invasion speed attenuated after the early 2000s in Tohoku (Figure 1h). It is assumed that the annual accumulated heat units required for completion of the sawyer's life cycle are insufficient in Northern Tohoku and that the contagious ability of the nematode is weakened in cold conditions there (Jikumaru & Togashi, 2000; Taketani, Okuda, & Hosoda, 1975). Given the immense historical damage of PWD in Japan and its likely future damage in world regions invaded more recently, there is a critical need to understand the processes driving PWD spread in order to make informed predictions of spread in the future.

One aspect of the population biology of PWD that possibly could play a role in the spread process is the Allee effect, which is the phenomenon of increasing per capita population growth with increasing density (Berec, Angulo, & Courchamp, 2007; Courchamp, Clutton-Brock, & Grenfell, 1999). There are several theoretical studies that predict the existence of Allee effects in the PWD system as a result

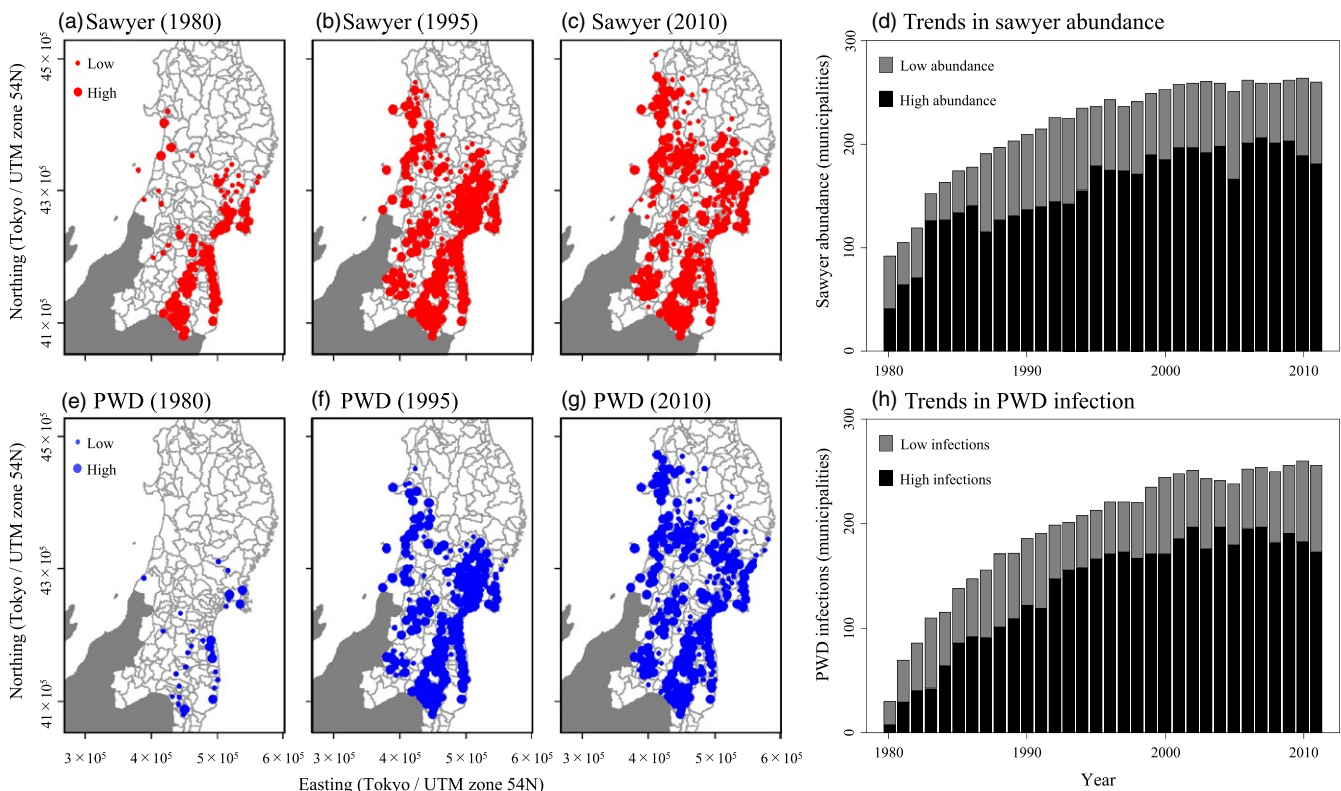


FIGURE 1 Trends in sawyer abundance and PWD infection. Sawyer abundances are in (a) 1980, (b) 1995 and (c) 2010, respectively. Small circles represent low values of sawyer abundance and large circles represent high abundance. PWD infection levels are in (e) 1980, (f) 1995 and (g) 2010, respectively. Small circles represent low abundance (1–100 infected pine trees) and the large one represent high abundance of infected trees (>100). Temporal trend of sawyer abundance (d) as the number of villages and of (h) PWD in Tohoku

of the need for two contacts by sawyers with trees. Consequently, sawyer and nematode population growth are positively related to the density of sawyers and density of healthy trees (Takasu et al., 2000; Togashi & Shigesada, 2006; Yoshimura et al., 1999). Adult sawyers feed on pine foliage in late spring and transmit nematodes from their body tissue to host trees. Nematodes proliferate inside trees resulting in reduced resin flow and weakening of trees. Sawyers are attracted to weakened trees where they lay eggs and larvae grow from summer to autumn. Prior to sawyer emergence from a pupal chamber, nematodes attach themselves to the sawyers, which thereby act as vectors in the next spring.

Theoretical studies indicate that Allee effects reduce spread rates (Lewis & Kareiva, 1993; Ovaskainen & Hanski, 2001) and can cause periodic invasion pulses (in heterogeneous habitats; Johnson, Liebhold, Tobin, & Bjørnstad, 2006) because substantial numbers of individuals are required to establish new populations ahead of the invasion front. We hypothesize that Allee effects influence invasion spread of PWD in conjunction with climatic conditions to slow rates of spread in cooler climates.

In this study, we analysed historical records of PWD spread through the Tohoku region during a 22-year period to explore the drivers of PWD range expansion. Ideally, modelling the spatial dynamics of this system could be accomplished with a spatially explicit population model of vector and pathogen dynamics (eg Yoshimura et al., 1999; Togashi & Shigesada, 2006). However, the data available from this region consisted of relatively crude records of none, low and high population levels and therefore such an approach was not possible. Instead, we modelled range expansion using a multistate occupancy model that accounted for observation errors (MacKenzie, Nichols, Seamans, & Gutiérrez, 2009; Veran et al., 2015). Our multistate occupancy model can be considered to be a density-structured version of stochastic patch occupancy models, that is SPOMs (Hanski & Thomas, 1994). Such density-structured models have previously been applied in numerical simulations exploring control strategies for invasive species in the presence of Allee effects (eg Taylor & Hastings, 2004), but rarely applied for data-model assimilation incorporating both demographic stochasticity and observation errors. Analysis using this model provided new understanding of how PWD spread is affected by dispersal of disease vectors and by climatic limitations and it provides a system for forecasting future spread in newly invaded regions.

2 | MATERIALS AND METHODS

2.1 | Data

Data on historical spread of PWD were collected annually by the Forest Conservation Departmental, Tohoku Forestry Research Institute Liaison Council from 1980 to 2011 (Forest Conservation Departmental Meeting of Tohoku Forestry Research Institute Liaison Council 2008, 2014; Figure 1). These data consisted of categorical records of the abundance of trees newly infected by PWD

and abundance of sawyers in each of 403 municipalities (eg villages) in the Tohoku region. Data were collected annually by two to seven individuals located in each of the six prefectures in the Tohoku region; these records can be visually inspected in Figure 1 and in Forest Conservation Departmental Meeting of Tohoku Forestry Research Institute Liaison Council (2008, 2014). The abundance of newly infected trees was categorized zero (0 infected trees/municipality), low (1–10 trees/municipality), medium (11–100 trees/municipality) and high (>100 trees/municipality). These categories reflected infection of both *Pinus densiflora* and *Pinus thunbergii* in each municipality. For the analyses reported here, we rescaled tree infection categories as zero (0 trees), low (1–100 trees) and high (>100 trees) because there were relatively few counts in the 1–10 and 11–100 categories in the original data. Surveys for sawyers were conducted using vane traps baited with α -pinene and ethanol deployed annually (Nakamura, 2008) and by debarking newly dead trees in each municipality and searching for sawyer galleries. Sawyer abundance was scaled from zero to high with zero indicating no sawyers detected either visually or with traps. Abundance values of low or high were roughly classified based upon expert interpretation by prefectural surveyors. There were no classification criteria published by surveyors and, therefore, we established classification probabilities to deal with this uncertainty (see Model section).

Meteorological data consisting of daily mean temperature and monthly number of days with rain at the geographical centroid of each municipality were extrapolated from AMeDAS (Automated Meteorological Data Acquisition System) weather station data using a distance weighted spatial interpolation method (Ishigooka, Kuwagata, Nishimori, Hasegawa, & Ohno, 2011; Seino, 1993). Because studies indicate that pines infected with nematodes remain asymptomatic at temperatures <15°C, the yearly summation of degree days above 15°C in each year was calculated at each municipality centroid (Taketani et al., 1975). We refer to this cumulative value as the *M. alternatus*–*B. xylophilus* index (MB index) after Taketani et al. (1975).

The most recent vegetation/land use map published by the Japan Integrated Biodiversity Information System (J-IBIS) (available online from http://www.biodic.go.jp/index_e.html) was used to calculate the total land area of pine vegetation (estimated as number of ~1 km × 1 km grid cells) in each municipality. The J-IBIS data are based on a national vegetation survey conducted from 1992 to 1996, which corresponds to the approximate midperiod of the 1980–2011 survey interval. Land area in each municipality was further classified into numbers of cells with coastal pines and number with inland pines because Japanese coastal pine woodlots are known to have from three to four times higher densities of trees than inland pine stands. Pines have historically been planted along the Japan sea coast to prevent strong ocean winds from penetrating into villages, but these stands are generally not managed for decades until they reach very high densities (Watanabe, Togashi, & Arai, 1987). All local environmental factors (ie MB index, monthly days with rain, area of inland pine forest and area of coastal pine forest) were standardized to values between 0 and 1.

2.2 | Model

Here, we applied a multistate occupancy model to the time series of sawyer abundance and tree mortality in the 403 municipalities ($s = 1, 2, \dots, 403$) from 1980 to 2011 ($t = 1980, \dots, 2011$) (Figure 2; MacKenzie et al., 2009; Veran et al., 2015). A multistate occupancy model is an extension of a simple occupancy model (MacKenzie, Nichols, Hines, Knutson, & Franklin, 2003) which specifies transition dynamics between only two categorical states such as presence/absence or breeding/nonbreeding. Occupancy models were developed to account for imperfect categorical classification; for example, we often recognize that “absence” is sometimes recorded despite the organism’s presence. This is particularly important because imperfect classification leads to underestimates of occupancy states and bias in the probabilities of transition between occupancy states in successive years (MacKenzie et al., 2003).

In our case, we accounted for transition between the three sawyer abundance states ($B_{s,t}^R = \text{zero, low or high}$) and three PWD infection states ($D_{s,t}^R = \text{zero, low or high}$). In general, (multistate) occupancy models consist of two subcomponents: observation models which express the probabilities of observed states being classified into true occupancy states with observation errors (ie Equation 1 and 2 in our model) and process models which express the transition dynamics between true occupancy states with demographic stochasticity (ie Equations 3–9 in our model). We use the term “true” occupancy states to refer to unobserved but actual occupancy states in contrast to “observed” states. Our motivation to use a multistate occupancy model is to infer the unbiased transition dynamics of sawyer and PWD infection from roughly

classified (but highly replicated) categorical data by explicitly modelling imperfect classification. Detailed structures and definitions of estimated variables in our model are presented in Figure 2 and Table 1.

Firstly, we define true occupancy states in our multistate occupancy model to account for imperfect classification of sawyer abundance and abundance of PWD-infected trees in each municipality. As with the recorded states, true sawyer abundance and true PWD infection levels were also categorized into three different states: $B_{s,t} = \text{zero, low or high}$ for sawyer abundance and $D_{s,t} = \text{zero, low or high}$ for PWD infection. Although several studies have modelled population abundances directly from observations measured as discrete categories (eg Royle & Nichols, 2003), our data did not allow us to estimate such continuous state variables. We did not have replicated observations from each site in a given year, which is critical to continuous estimation. Using multinomial probability distributions, we parameterized probabilities of recording each state j (ie columns) given that the true state is i (ie rows) as follows: for sawyer abundance,

$$\eta_k^{[ij]} = \begin{matrix} \text{zero} & \text{low} & \text{high} \\ \text{zero} & \begin{bmatrix} 1 & 0 & 0 \\ 1-p_k^{[\text{low}]} & p_k^{[\text{low}]} & 0 \\ 0 & 1-p_k^{[\text{high}]} & p_k^{[\text{high}]} \end{bmatrix} \\ \text{low} & & \\ \text{high} & & \end{matrix} \quad (1)$$

where $p_k^{[i]}$ is the classification probability for recording without observation errors at (true) infection state k , and for PWD infection levels,

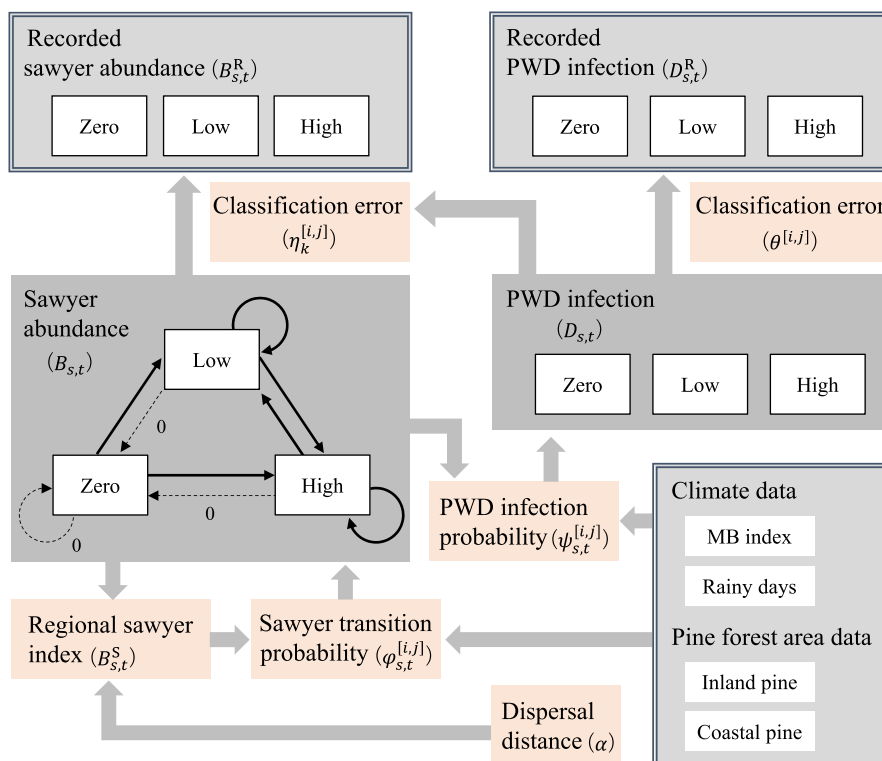


FIGURE 2 Schematic diagram of the model structure [Colour figure can be viewed at wileyonlinelibrary.com]

TABLE 1 Descriptions of unknown variables in our multistate occupancy model. Prior probabilities were required for some variables in the process of the assimilation (the column of “Priors”). The other variables were derived from Equations 1–9 in the main text. Note that all unknown variables were estimated simultaneously

Variables	Descriptions	Priors
$B_{s,t}$	Sawyer abundance states (zero, low or high) at municipality s in year t	Multinomial distribution <i>Multin</i> (1/3,1/3,1/3)
$D_{s,t}$	Pine wilt disease (PWD) infection states (zero, low or high) at municipality s in year t	Multinomial distribution <i>Multin</i> (1/3,1/3,1/3)
$r_k^{[ij]}$	Probability of recording sawyer abundance state j given true state i for (true) PWD infection level k	–
$\theta^{[ij]}$	Probability of recording PWD infection state j given true state i	–
$p_k^{[i]}$	Classification probabilities for recording sawyer abundance state i without observation errors at PWD infection state k	Beta distribution <i>Beta</i> (1,1)
$q^{[i]}$	Classification probabilities for recording PWD infection state i without observation errors	Beta distribution <i>Beta</i> (1,1)
$B_{s,t}^S$	Regional sawyer abundance index	–
$w_{s,s'}$	Spatial weight matrix expressed by the exponential decay function of distance between municipalities s and s'	–
α	Average dispersal distance of sawyers per year	Uniform distribution <i>Unif</i> (0,20)
c	Relative dispersing sawyer abundance for low abundance category	Uniform distribution <i>Unif</i> (0,1)
$\varphi_{s,t}^{[ij]}$	Sawyer transition probability from state i to state j between year t and $t+1$ at municipality s	–
$\psi_{s,t}^{[ij]}$	Probability of PWD infection state j given the sawyer abundance state i at municipality s in year t	–
$b_{ij,k}^B$	Intercept or coefficient of each explanatory variables for the multinomial regression of sawyer transition probability	Gaussian distribution <i>Norm</i> (0,100 ²)
$b_{ij,k}^D$	Intercept or coefficient of each explanatory variables for the multinomial regression of PWD infection probability	Gaussian distribution <i>Norm</i> (0,100 ²)

$$\theta^{[ij]} = \begin{matrix} & \begin{matrix} \text{zero} & \text{low} & \text{high} \end{matrix} \\ \begin{matrix} \text{zero} \\ \text{low} \\ \text{high} \end{matrix} & \begin{bmatrix} 1 & 0 & 0 \\ 1 - q^{[\text{low}]} & q^{[\text{low}]} & 0 \\ 0 & 1 - q^{[\text{high}]} & q^{[\text{high}]} \end{bmatrix} \end{matrix} \quad (2)$$

where $q^{[i]}$ is the classification probability of recording without observation errors. If the classification probability is 1, our survey data are completely classified without observation errors. Otherwise (ie $0 \leq p_k^{[i]}, q^{[i]} < 1$), our survey data are affected by imperfect classifications. In Equation 1, we assumed that the classification probabilities for sawyer abundances were different if the PWD infection state was different ($p_{\text{zero}}^{[\text{low}]} \neq p_{\text{low}}^{[\text{low}]} \neq p_{\text{high}}^{[\text{low}]}$ and $p_{\text{zero}}^{[\text{high}]} \neq p_{\text{low}}^{[\text{high}]} \neq p_{\text{high}}^{[\text{high}]}$). This was because we expected that true PWD infection levels affect the measurement of sawyer abundance from pheromone traps. At high infection levels, adult sawyers feed on large amounts of pine foliage resulting in the release of large amounts of natural attractants which compete with monitoring traps (Mota et al., 2009).

Next, we define a regional sawyer abundance index, which quantifies the immigration of sawyers from surrounding municipalities ($s \neq s'$) and from the local municipality ($s = s'$). This regional sawyer abundance index, $B_{s,t}^S$, is defined as:

$$B_{s,t}^S = \sum_{s'=1}^{403} w_{s,s'} \Phi(B_{s',t}) \quad (3)$$

where $w_{s,s'}$ is a spatial weight matrix expressed by the exponential decay function of distance between municipalities, $d_{s,s'}$, and average dispersal distance of sawyers per year, α :

$$w_{s,s'} = \exp(-d_{s,s'}/\alpha) / \sum_{s'=1}^{403} \exp(-d_{s,s'}/\alpha). \quad (4)$$

The exponential dispersal kernel, which is controlled by a single parameter, α , is employed here because of its simplicity. It should be noted that results were qualitatively the same as those derived from applying a Gaussian dispersal kernel (results not shown). $\Phi(B_{s',t})$ is the function which estimates the number of sawyers dispersing from each municipality s' :

$$\Phi(B_{s',t}) = \begin{cases} 0 & \text{if } B_{s',t} = \text{zero} \\ c & \text{if } B_{s',t} = \text{low} \\ 1 & \text{if } B_{s',t} = \text{high} \end{cases} \quad (5)$$

We also define a new constant parameter c ($0 < c < 1$), which converts the lowest category of sawyer abundance ($B_{s',t} = \text{low}$) into the relative abundance of sawyers in municipality s' assuming that the high sawyer abundance ($B_{s',t} = \text{high}$) equals $\Phi(B_{s',t}) = 1.0$. Note that we set the upper bound of sawyer abundance ($\Phi(B_{s',t})$) to 1.0. This allowed us to derive relative immigration of sawyers from our categorical records. Under these conditions, regional sawyer abundance

index, $B_{s,t}^S$ can vary from 0, regionally zero abundance, to 1.0, regionally high abundance.

For sawyer dynamics, we consider the transition from one state i (=zero, low, or high) to another j (=zero, low, or high) between years t and $t + 1$ using a transition probability matrix, $\varphi_{s,t}^{[ij]}$ (Figure 2). In our model, we tested whether the transition probabilities were influenced by local environmental factors (MB index, $X_{s,t}^{mb}$; monthly days with rain, $X_{s,t}^{rd}$; area of inland pine forest, $X_{s,t}^{lp}$; area of coastal pine forest, $X_{s,t}^{cp}$) and regional sawyer abundance index ($\log B_{s,t-1}^S$), in the previous year. We used flexible multinomial regression models to describe complex transition dynamics with three categorical states; then, we let $\varphi_{s,t}^{[ij]}$ be defined as follows: if $j \neq \text{zero}$,

$$\varphi_{s,t}^{[ij]} = \frac{\exp(\beta_{ij}^B \mathbf{X}_{s,t}^B)}{1 + \exp(\beta_{i,\text{low}}^B \mathbf{X}_{s,t}^B) + \exp(\beta_{i,\text{high}}^B \mathbf{X}_{s,t}^B)} \quad (6)$$

and if $j = \text{zero}$,

$$\varphi_{s,t}^{[i,\text{zero}]} = 1 - \varphi_{s,t}^{[i,\text{low}]} - \varphi_{s,t}^{[i,\text{high}]} \quad (7)$$

where $\mathbf{X}_{s,t}^B = \{1, X_{s,t}^{mb}, X_{s,t}^{rd}, X_{s,t}^{lp}, X_{s,t}^{cp}, \log B_{s,t-1}^S\}$ and $\beta_{ij}^B = \{b_{ij,\text{intercept}}^B, b_{ij,\text{mb}}^B, b_{ij,\text{rd}}^B, b_{ij,\text{lp}}^B, b_{ij,\text{cp}}^B, b_{ij,\text{rs}}^B\}$. In Equation 6, $b_{ij,k}^B$ are the intercept and coefficients for each local environmental factor or regional sawyer abundance index. Because our model uses zero abundance ($j = \text{zero}$) as a reference state in Equation 7, a positive or negative $b_{ij,k}^B$ means that the focal variable k promotes or inhibits, respectively, the transition from the i to j abundance states more than to the zero abundance state. Observed transitions occurring in municipalities within 20 km from the southern boundary (the set of municipalities which is expressed by s^{FS}) were ignored in the estimation of transition probabilities (ie Equation 13) because the sawyer populations in these municipalities were likely influenced by sawyer populations outside of the Tohoku area and their inclusion would risk biased estimation.

Finally, we consider the probability, $\psi_{s,t}^{[ij]}$, of PWD infection state j (=zero, low or high) given that the sawyer abundance state is i (=zero, low, or high). If sawyer abundance state is zero ($i = \text{zero}$), then no occurrence is assumed. As done for transition probabilities for sawyer abundance states, we tested whether the PWD infection probabilities were influenced by local environmental factors. With multinomial regression models, we let $\psi_{s,t}^{[ij]}$ be defined as follows: if $j \neq \text{zero}$,

$$\psi_{s,t}^{[ij]} = \frac{\exp(\beta_{ij}^D \mathbf{X}_{s,t}^D)}{1 + \exp(\beta_{i,\text{low}}^D \mathbf{X}_{s,t}^D) + \exp(\beta_{i,\text{high}}^D \mathbf{X}_{s,t}^D)} \quad (8)$$

and if $j = \text{zero}$,

$$\psi_{s,t}^{[i,\text{zero}]} = 1 - \psi_{s,t}^{[i,\text{low}]} - \psi_{s,t}^{[i,\text{high}]} \quad (9)$$

where $\mathbf{X}_{s,t}^D = \{1, X_{s,t}^{mb}, X_{s,t}^{rd}, X_{s,t}^{lp}, X_{s,t}^{cp}\}$ and $\beta_{ij}^D = \{b_{ij,\text{intercept}}^D, b_{ij,\text{mb}}^D, b_{ij,\text{rd}}^D, b_{ij,\text{lp}}^D, b_{ij,\text{cp}}^D\}$ which represents the intercept and coefficients for local environmental factors. In our model, we account only for the influence of sawyer abundance on PWD infection level but not that of PWD

infection level on sawyer abundance. When the latter effect was included in the model, the Markov chain never converged; we suspect that this may be due in part from the variable management (sanitation cutting of infected trees) among municipalities which would influence numbers of beetles produced following PWD infection, although data on management effort were lacking. We should also note that pine forest area did not vary through time in our model because data describing the dynamics of total pine forest area were lacking. Thus, we used the static constant of the inland and coastal pine forest area as only a rough proxy of healthy pine abundances.

2.3 | Model assimilation

Using the Markov chain Monte Carlo (MCMC) method, we drew samples from the following joint posterior distribution for true state variables (\mathbf{B} and \mathbf{D}) and unknown parameters (\mathbf{b}^B , \mathbf{b}^D , \mathbf{p} , \mathbf{q} , α , c) conditional on the recorded time-series data (\mathbf{B}^R and \mathbf{D}^R), the environmental data (\mathbf{X}) and the distance data between municipalities (\mathbf{d}):

$$\begin{aligned} & p(\mathbf{B}, \mathbf{D}, \mathbf{b}^B, \mathbf{b}^D, \mathbf{p}, \mathbf{q}, \alpha, c | \mathbf{B}^R, \mathbf{D}^R, \mathbf{X}, \mathbf{d}) \\ & \propto f_B(\mathbf{B}_{1980}^R | \mathbf{B}_{1980}, \mathbf{D}_{1980}, \mathbf{p}) f_D(\mathbf{D}_{1980}^R | \mathbf{D}_{1980}, \mathbf{q}) g_B^{\text{Init}}(\mathbf{B}_{1980}) g_D^{\text{Init}}(\mathbf{D}_{1980}) \\ & \times \prod_{t=1981}^{2011} f_B(\mathbf{B}_t^R | \mathbf{B}_t, \mathbf{D}_t, \mathbf{p}) f_D(\mathbf{D}_t^R | \mathbf{D}_t, \mathbf{q}) g_B^{\text{FS}}(\mathbf{B}_t) g_B(\mathbf{B}_t | \mathbf{B}_{t-1}, \phi) g_D(\mathbf{D}_t | \mathbf{D}_t, \psi) \\ & \times \pi(\mathbf{b}^B) \pi(\mathbf{b}^D) \pi(\mathbf{p}) \pi(\mathbf{q}) \pi(\alpha) \pi(c) \end{aligned} \quad (10)$$

where f_B and f_D are the probability mass functions (PMF) for the observation models, and g_B and g_D are the PMFs for the process models of sawyer abundance and PWD infection at year t , respectively:

$$f_B(\mathbf{B}_t^R | \mathbf{B}_t, \mathbf{D}_t, \mathbf{p}) = \prod_{s=1}^{403} \eta_{D_{s,t}}^{[B_{s,t}, B_{s,t}^R]} \quad (11)$$

$$f_D(\mathbf{D}_t^R | \mathbf{D}_t, \mathbf{q}) = \prod_{s=1}^{403} \theta_{D_{s,t}}^{[D_{s,t}, D_{s,t}^R]} \quad (12)$$

$$g_B(\mathbf{B}_t | \mathbf{B}_{t-1}, \phi) = \prod_{s \notin s^{FS}} \phi_{s,t}^{[B_{s,t-1}, B_{s,t}]} \quad (13)$$

$$g_D(\mathbf{D}_t | \mathbf{D}_t, \psi) = \prod_{s=1}^{403} \psi_{s,t}^{[D_{s,t-1}, D_{s,t}]} \quad (14)$$

g_B^{FS} , g_B^{Init} , g_D^{Init} and π are the prior distributions for occupancy states (g_B^{FS} , sawyer states in the southern most municipalities $s \in s^{FS}$; g_B^{Init} , sawyer states in the initial year $t = 0$; g_D^{Init} , PWD infection states in the initial year $t = 0$) or the other parameters (π , parameters of the observation and process models). We assigned vague priors for all variables (Table 1). At each MCMC iteration, each known variable updates by calculating its related PMFs and priors. For example, calculations of the second PMF (ie Equation 12) and the prior $\pi(\mathbf{p})$ is required for the update of $p_k^{[i]}$. It is noteworthy that all the unknown parameters were simultaneously fitted and we never fitted any parameters independently.

We ran three independent MCMC chains and retained 30,000 iterations after an initial burn-in of 30,000 iterations. We then retained the samples every 30th iterations. The convergence of MCMC samples was confirmed by monitoring the trace plots and checking the Gelman–Rubin diagnostic $\hat{R} < 1.1$ for each parameter. Our analysis was conducted using R 3.3.1 (R Core Team 2017) and JAGS 4.2.0 (Plummer, 2003).

3 | RESULTS

During the period 1980–2011, there was a general wave of increasing sawyer abundance and increasing PWD infection levels that moved from the south to the north (Figure 1). Based upon 90% quantile regression (R package “QUANTREG”), the rate of spread of nonzero sawyer abundance was estimated as 3.14 km/year (95% confidential interval: 2.07–4.48), spread of high sawyer abundance was 2.13 km/year (1.54–3.01), spread of low PWD infection was 2.57 km/year (2.24–3.07) and spread of high PWD was 3.09 km/year (2.77–3.62) (Figure 3). Increases in sawyer abundance generally preceded increases in PWD infection (Figure 3). There was some evidence of attenuation in expansion of both sawyer populations and PWD infection levels as the disease spread northward (Figure 1d,h).

Figure 4 shows the estimation of the classification probability matrix $\eta_k^{[i,j]}$, which evaluates misclassification of the true sawyer abundance state from the observed state under each PWD infection state (Figure 4a), and $\theta^{[i,j]}$, which evaluates the misclassification of the true PWD infection state from the observed level (Figure 4b). For $\eta_k^{[i,j]}$, the

classification probabilities at the low sawyer state were $p_{\text{zero}}^{[\text{low}]} = 0.79$ [0.68, 0.88], $p_{\text{low}}^{[\text{low}]} = 0.91$ [0.89, 0.92] and $p_{\text{high}}^{[\text{low}]} = 0.83$ [0.77, 0.88] (medians and 95% credible intervals) when PWD infection was zero, low and high, respectively (Figure 4a, Appendix: Table S1). Conversely, the classification probabilities at the high abundance sawyer state were estimated to be near 1.0 for any PWD infection states ($p_{\text{zero}}^{[\text{high}]} = 0.99$ [0.96, 1.000], $p_{\text{low}}^{[\text{high}]} = 0.98$ [0.94, 1.00] and $p_{\text{high}}^{[\text{high}]} = 0.99$ [0.99, 0.99]). These results can be interpreted that there are greater possibilities of misclassification at low sawyer abundance than at high abundance. This is intuitively interpretable as it is more difficult to detect sawyers as the true population size gets smaller. For $\theta^{[i,j]}$, the classification probabilities at low and high states were $q^{[\text{low}]} = 0.74$ [0.71, 0.79] and $q^{[\text{high}]} = 0.92$ [0.91, 0.93], respectively (Figure 4b, Appendix: Table S1). This means that in actual PWD surveys, observations are not accurate when symptoms of PWD are not advanced and numbers of sawyers are low. Some type of statistical treatment which accounts for stochastic uncertainty, such as our multistate occupancy model, is necessary for meaningful interpretation of survey data.

We found significant effects of local environmental factors on the dynamics of the (true) sawyer abundance level (Figure 5a–e, Appendix: Table S2). The MB index promoted the transition from low to high states ($b_{\text{low,high,mb}}^{\text{B}} = 1.915$ [0.038, 3.875] and $b_{\text{high,low,mb}}^{\text{B}} = -6.149$ [−12.91, −0.407], Figure 5a). High inland pine forest areas appeared to sustain pandemic states ($b_{\text{high,high,lp}}^{\text{B}} = 58.71$ [8.424, 217.5], Figure 5c) while we could not find a strong effect of coastal pine forest area (Figure 5d). Although the effects of monthly days with rain on sawyer dynamics were complicated, more rainy days generally

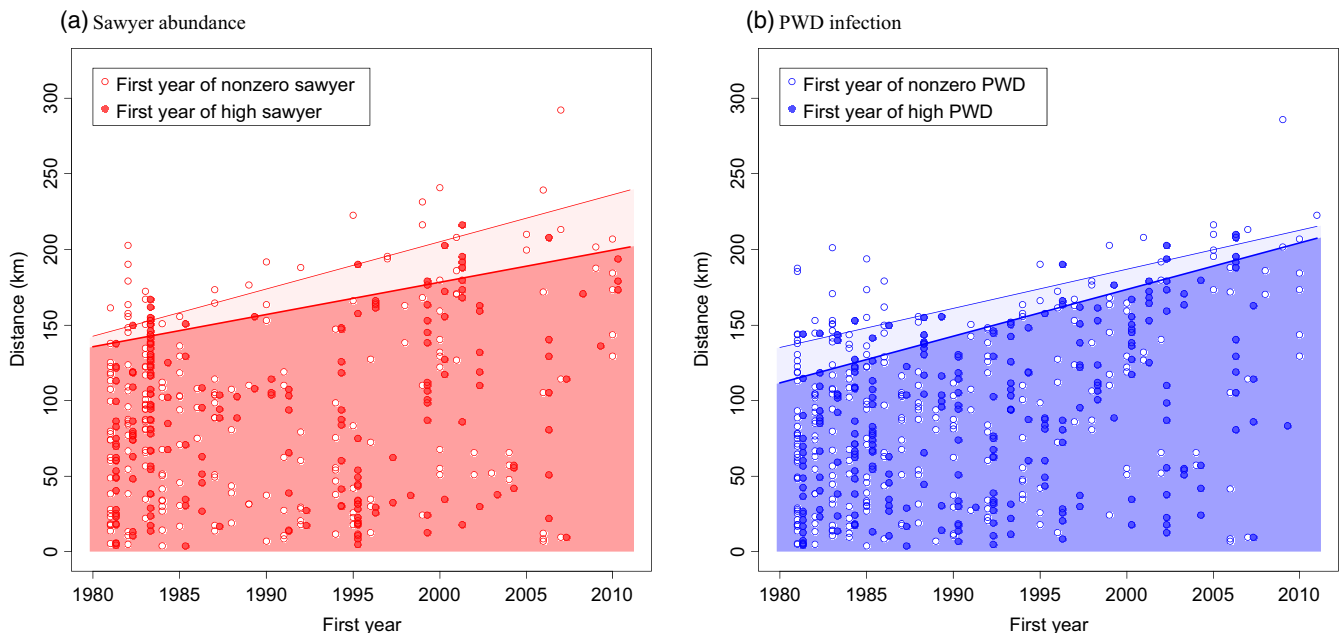
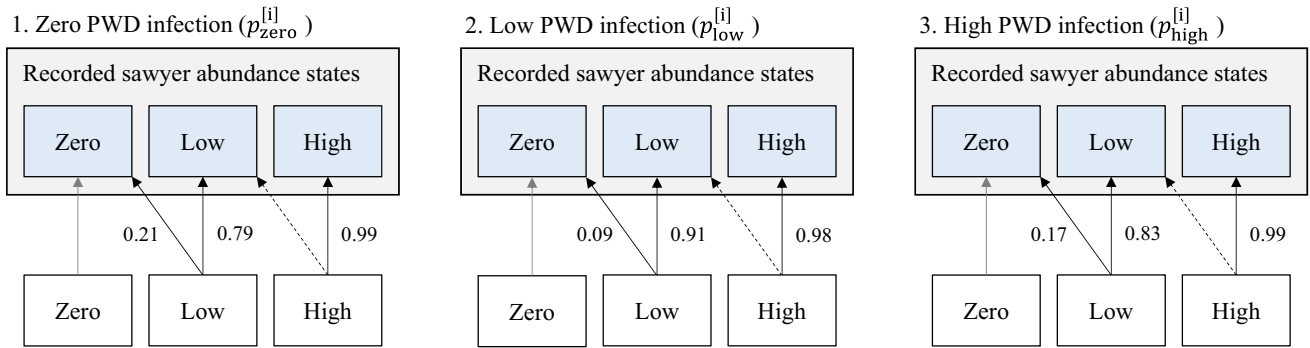


FIGURE 3 Quantile regression (90th percentile) for distance as a function of year of first nonzero (a) sawyer abundance and (b) PWD abundance. The light shaded area with pink and the upper line in Figure 3a are the 90% quantile and the quantile regression lines of the first year of nonzero sawyer abundance. The red shaded area and the lower line are for the first year of high sawyer abundance. The area with light blue and the upper line in Figure 3b are for the first year of nonzero PWD infection. The blue shaded area and the lower line are for the first year of high PWD infections

(a) Sawyer abundance



(b) PWD infection ($q^{[I]}$)

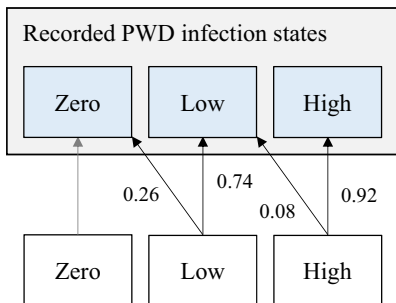


FIGURE 4 Classification probabilities as for the observation errors. Note that the probabilities shown are median values. The probabilities of insignificance are drawn with dotted arrows and those in grey are fixed values (ie = 1.0) [Colour figure can be viewed at wileyonlinelibrary.com]

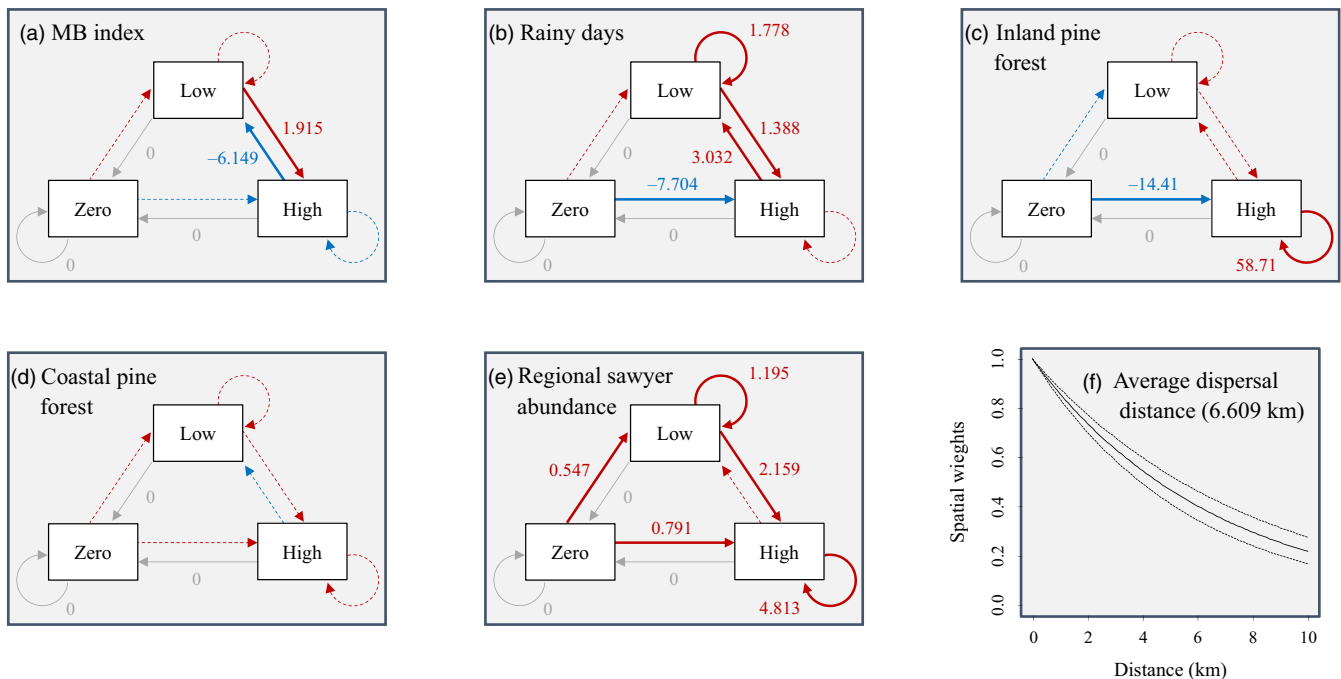


FIGURE 5 Effects of predictors on local sawyer abundance states (a–e) and estimated dispersal distance α (f). The red and blue arrows represent the positive and negative effects of the origins on the terminals. The numbers shown are median estimates of statistically significant while those of insignificant were not shown. The zero values are set for all the effect to zero states so that the transition rates can be compatible with each other

promoted the transition from high to low states ($b_{\text{high,low,rd}}^B = 3.032$ [0.188, 6.530] vs. $b_{\text{low,high,rd}}^B = 1.388$ [0.198, 2.543], and $b_{\text{low,low,rd}}^B = 1.778$ [0.745, 2.868], Figure 5b). In Figure 5e, increasing regional sawyer abundance promoted the transition from zero to low states ($b_{\text{zero,low,rs}}^B = 0.547$ [0.458, 0.652]), from low to high ($b_{\text{low,high,rs}}^B = 2.159$ [1.362, 3.181]) and from zero to high ($b_{\text{zero,high,rs}}^B = 0.791$ [0.521, 1.172]). All the transition rates from low to high are positive, and moreover, sawyer population at sparse states had the lower probabilities of transition to high states than did higher abundance population, even for the same regional abundance index ($b_{\text{zero,high,rs}}^B < b_{\text{low,high,rs}}^B < b_{\text{high,high,rs}}^B$). This suggests the existence of positive density dependence in the sawyer dynamics, that is the existence of an Allee effect.

Average sawyer dispersal distance in Tohoku was estimated to be 6.609 km/year (α : [5.662, 7.812], Figure 5f, Appendix: Table S2). Takasu et al. (2000) reported that the average dispersal distance was 4.2 km/year based upon analysis of historical PWD invasion records and was 1.82 km/year based upon mark-recapture experiments using sawyers. Our value of 6.609 km/year is higher than those reported by Takasu et al. (2000) but within the same order of magnitude.

Using these estimates, we investigated the effect size of the regional sawyer abundance and temperature constraints, that is MB index, on the transition probability between (local) sawyer abundance states in Figure 6. The transition probability matrix $\phi_{s,t}^{[i,j]}$ in Equations 6 and 7 was recalculated substituting low and high

abundances of regional sawyer populations (parameter $c = 0.254$ [0.133, 0.403] and 1, respectively) and also low and high MB indexes (474 and 711 day degrees, respectively). We used 25% and 75% quantiles as values for low and high MB indices, which fall below and exceed the thermal requirement for postdiapause larval development of sawyers (540 day degrees; Igarashi, 1977).

As shown in Figure 5e, high regional abundance supports the continuation of high abundances in municipalities compared with zero and low abundance in municipalities (Figure 6, right panels). In contrast, the MB index had less effect on local sawyer abundance than did regional abundances. Although high MB index values slightly increased probabilities of sustaining high abundances and increased probabilities of populations increasing from low to high abundances (Figure 6, compare upper to lower panels), it was not prominent in comparison with the effect of regional abundance (Figure 6, compare left to right panels). Therefore, we suspect that regional sawyer abundance is the primary driver of local sawyer dynamics and that the MB index more subtly affects populations. It should be noted that high sawyer abundances have higher probabilities of transitioning to zero in the next year in the presence of low regional abundance and high MB index (the right bar in Figure 6, left-bottom panel). Although we could not model the dynamics between healthy pine forest area and PWD infection level, suitable climatic conditions may facilitate the crash of sawyer populations which consequently causes the depletion of host resources in nature.

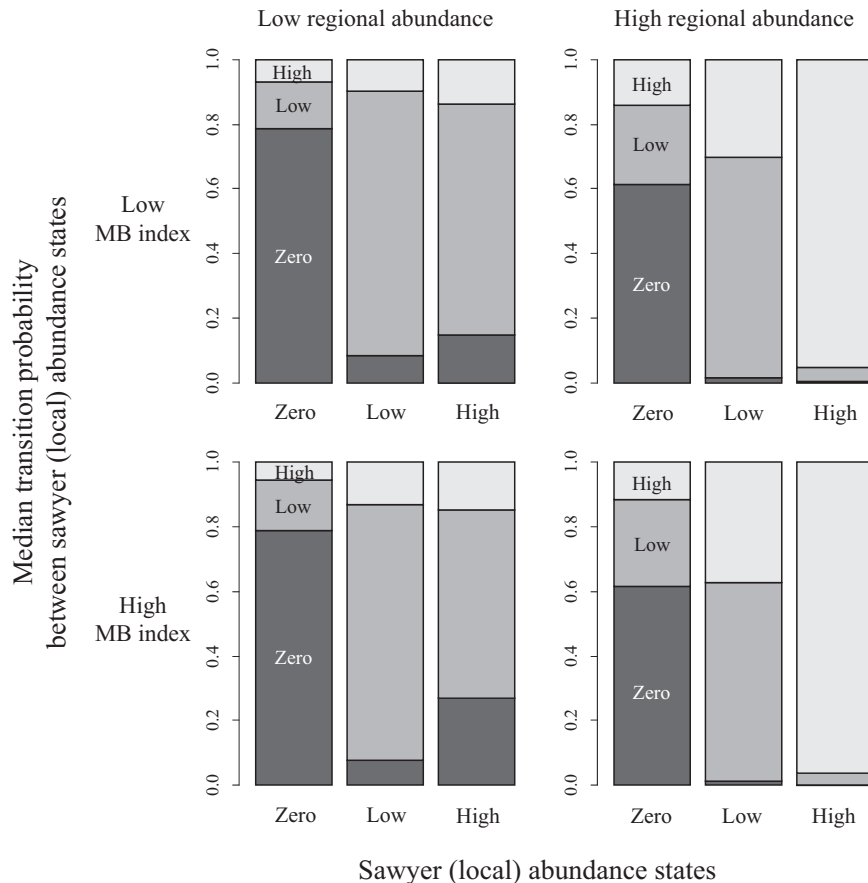


FIGURE 6 Transition probability of the sawyer density index. The environmental values were categorized by low ($B_{s,t}^S = c$) and high ($B_{s,t}^S = 1$) regional density and by low ($X_{s,t}^{\text{mb}} = 474$) and high MB ($X_{s,t}^{\text{mb}} = 711$) index, and the probability is calculated by Equations 6 and 7

We also found significant effects of local environmental factors on PWD occurrence (Figure 7, Appendix: Table S3). The MB index and inland pine forest area positively enhanced the probability of PWD incidence ($b_{ij,mb}^D > 0$ and $b_{ij,lp}^D > 0$ in most case), while monthly days with rain and coastal pine forest area reduced probabilities ($b_{ij,rd}^D < 0$ and $b_{ij,cp}^D < 0$). These effects were consistent across all sawyer abundance states.

4 | DISCUSSION

Even though sawyer populations are native to the entirety of Japan, the invasion of PWD creates a wave of elevated sawyer abundance that generally precedes the invading wave of PWD infections (Figures 1 and 3). This is because there is a positive feedback operating between the infectious nematode and its sawyer vector. Infection of host trees by nematodes creates declining trees, which comprise a resource for sawyers which exploit these trees and then disperse from them in large numbers. Elevated sawyer populations result in increased transmission of nematodes and the nematodes increase in abundance and are able to invade new areas with dispersing sawyers (Togashi & Shigesada, 2006).

The pattern of an increasing positive effect of sawyer abundance on sawyer population growth with increasing sawyer abundance provides evidence of an Allee effect (Figure 5e) in this system. Yoshimura et al. (1999) previously reported the existence of an Allee effect in the PWD system but that observation was derived from a very limited area (920 m²). Our results demonstrate that Allee effects are prominent across a broader regional scale. Based upon theoretical studies (Keitt, Lewis, & Holt, 2001; Lewis & Kareiva, 1993), we conclude that this Allee effect reduces rates of PWD spread. Specifically, we postulate that the Allee effect observed in this system may have been responsible, in part, for the decrease in invasion speed observed in the early 2000s (Figure 1). Although we anticipated that climatic constraints, that is, the MB index, made a substantial contribution in slowing the invasion in northern regions,

it actually appears to have had a much weaker effect on sawyer dynamics than did regional sawyer abundance (Figure 6).

Theoretical studies by Keitt et al. (2001) showed that the presence of an Allee effect may limit the ability of invading species to spread and establish in areas at the periphery of suitable environments, a phenomenon termed “range pinning” because the invading species cannot persist below a critical population density known as an “Allee threshold.” We anticipate that the Allee effect in this system may be limiting PWD populations from expanding to the boundary of suitable habitat to the north. Studies of other pest species, for example *Lymantria dispar* (Erebidae; Lepidoptera), reported that emigration must be sufficient to overcome the negative effects of Allee effects on population growth in order to expand their range (Johnson et al., 2006; Tobin, Whitmire, Johnson, Bjørnstad, & Liebhold, 2007).

Considering the secondary effect of MB index in our analyses, it may be biologically possible for PWD to eventually overcome Allee effects and expand its range further to the north. Careful surveillance should be kept for the sudden expansion of PWD in the northern front in Tohoku. Furthermore, our results suggest that pest control methods which can strengthen Allee effects might be an effective strategy for limiting the growth and spread of populations along the expanding population front (Yamanaka & Liebhold, 2009). Sanitation logging of newly infected host trees might be a possible approach for accomplishing this (Yoshida, 2006).

By fitting historical data to our mechanistic model, we obtained an indirect estimate of the average sawyer dispersal distance ($\alpha = 6.609$ km/year). This estimate is potentially useful in informing local governments implementing host removal buffer zone strategies for containment of PWD. Our estimate is larger than those reported by Takasu et al. (2000) (4.2 km/year from historical invasion records for PWD and 1.82 km/year using mark-recapture experiments with sawyers). The rate of spread of PWD’s range over pine stands has been determined in several areas by mapping the expanding population front of PWD incidence over 9 years and the speed ranged from 2–3 km/year to 9–10 and 3–15 km/year (Togashi,

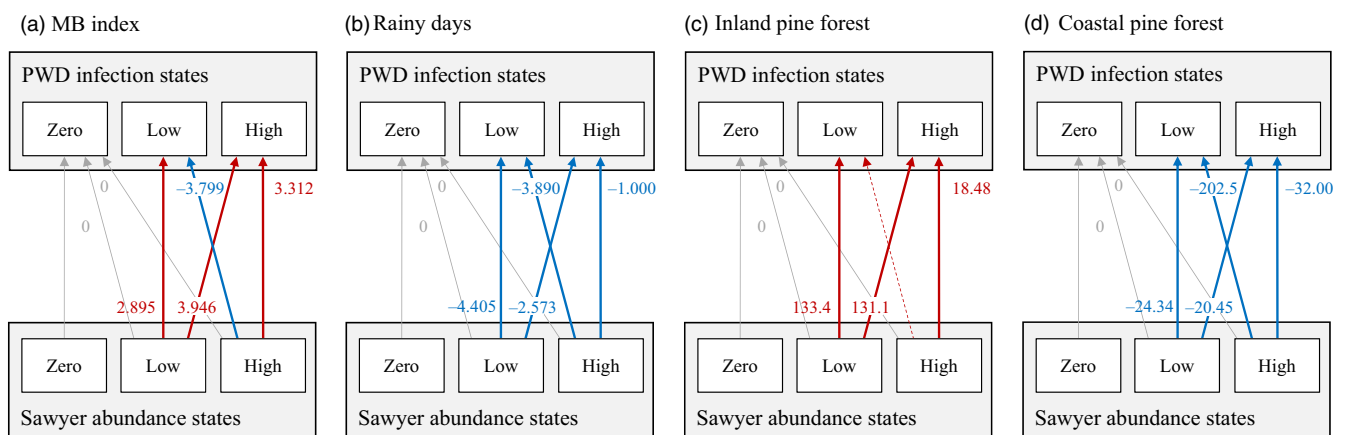


FIGURE 7 Effects of predictors on local PWD infection level. The red and blue arrows represent the positive and negative effects of the origins on the terminals

2008). Our estimate of 6.609 km/year is reasonable because mark-recapture experiments sometimes fail to detect long-distance dispersal (Turchin & Thoeny, 1993). Furthermore, theory predicts that observed spread rates will be lower on average when populations are affected by a strong Allee effect (Lewis & Kareiva, 1993) because small populations arising via long-range dispersal are driven to extinction.

We found that the local area of inland pine forest had a strong effect sustaining high beetle abundance (Figure 5c) and these elevated sawyer abundances contributed to increases in PWD infection (Figure 7c). In contrast, coastal pine forest area did not influence beetle abundance (Figure 5d) and negatively influenced the effect of sawyer densities on PWD infection (Figure 7d). This is a counterintuitive result and we do not have a plausible biological explanation. It is possible that this reflects the coarse spatial resolution of data; the number of grid cells of coastal pine forests is much smaller than for inland pine forest, c.a. 16% on average, and coastal pine forests are only located in municipalities with coastlines. The sparse and geographically constrained incidence of coastal pine forests might result in confounding of unobserved environmental limitation factors. If we had access to data on pine density in addition to numbers of grid cells with pines, the role of coastal pine forest might have been more clearly elucidated. Future updates in J-IBIS (http://www.biodic.go.jp/index_e.html) may provide sufficient data for additional analyses.

We also identified important information about meteorological influences in this system. Numbers of rainy days negatively affected PWD infection rates (Figure 7b). Sata (1942) observed that numbers of symptomatic pines rapidly increased during summer drought conditions but changed very little during cool and rainy summers. Pines may be physiologically less resistant to PWD infection during summer droughts. Heavy rain (above 5 mm/hr) may constrain adult dispersal behaviour (Kishi, 1995). It also should be noted that observation errors are greater when sawyer abundance and PWD infections are low (Figure 4). This suggests a need to improve surveillance quality during periods of PWD latency, perhaps through the additional sampling.

The analysis presented here demonstrates the utility of the application of a multistate occupancy model through the use of computer-intensive assimilation. It is doubtful that we could have successfully detected the clear presence of an Allee effect in sawyer populations from these very coarse categorical data using traditional methods (eg linear models). This type of crude pest surveillance data are often collected over long periods for various pest species, but data quality issues typically limit their utility for model fitting (eg Johnson et al., 2006; Yamanaka, Nelson, Uchimura, & Bjørnstad, 2012). The multistate occupancy model applied here potentially could be applied to other systems where such previously overlooked data might exist and have great potential to provide important insight not only to questions related to practical pest management but also for answering basic ecological problems. Moreover, with this model, it should be possible to predict the future expansion of PWD in Tohoku though such an

exercise is beyond the scope of this study. It may also be possible to predict PWD spread elsewhere in East Asia or in Europe using comparable meteorological and vegetation data in addition to comparable PWD and sawyer data describing current conditions. In addition, it might be possible in the future to use this model to evaluate, via simulation, the effects of PWD management such as sanitation logging.

ACKNOWLEDGEMENTS

We thank Dr. Katsunori Nakamura and Dr. Toshinori Maehara and Dr. Takuma Takanashi for their kind help sharing the information of PWD in Tohoku. We also thank Dr. Daisuke Kyogoku for useful advice in statistical analyses. Our collaboration was supported by JSPS Short-Term Fellowship No. S10090 for A.M.L. and the travel support to A.M.L. by the Society of Population Ecology.

AUTHORS' CONTRIBUTIONS

T. Yamanaka, E.S.-K. and A.M.L. set up the bases of the analyses. T. Yamanaka, T. Yamakita and Y.O. discussed the framework of our model. Y.O. constructed multioccupancy model, and Y.O. and T. Yamanaka executed the assimilation. E.S.-K. and A.M.L. discussed the biological interpretations of our results. All authors contributed to the writing of the manuscript.

DATA ACCESSIBILITY

The data used in the study are available from the Dryad Digital Repository: <https://doi.org/10.5061/dryad.61c4h39> (Osada, Yamakita, Shoda-Kagaya, Liebhold, & Yamanaka, 2018). The original records, from which we extracted our data, can be found in the FFPRI repository (<https://www.ffpri.affrc.go.jp/pubs/bulletin/433/documents/433-9.pdf>) (Forest Conservation Departmental Meeting of Tohoku Forestry Research Institute Liaison Council, 2008, 2014).

ORCID

Yutaka Osada  <http://orcid.org/0000-0001-5967-194X>

Takehisa Yamakita  <http://orcid.org/0000-0002-5451-1231>

Etsuko Shoda-Kagaya  <http://orcid.org/0000-0003-4705-4033>

Andrew M. Liebhold  <http://orcid.org/0000-0001-7427-6534>

Takehiko Yamanaka  <http://orcid.org/0000-0003-2888-1076>

REFERENCES

- Berec, L., Angulo, E., & Courchamp, F. (2007). Multiple Allee effects and population management. *Trends in Ecology and Evolution*, 22, 185–191. <https://doi.org/10.1016/j.tree.2006.12.002>
- Courchamp, F., Clutton-Brock, T. H., & Grenfell, B. T. (1999). Inverse density dependence and the Allee effect. *Trends in Ecology and Evolution*, 14, 405–410. [https://doi.org/10.1016/S0169-5347\(99\)01683-3](https://doi.org/10.1016/S0169-5347(99)01683-3)

- Evans, H. F., McNamara, D. G., Braasch, H., Chadoeuf, J., & Magnusson, C. (1996). Pest Risk Analysis (PRA) for the territories of the European Union (as PRA area) on *Bursaphelenchus xylophilus* and its vectors in the genus *Monochamus*. *EPPO Bulletin*, 26, 199–249. <https://doi.org/10.1111/j.1365-2338.1996.tb00594.x>
- Forest Conservation Departmental Meeting of Tohoku Forestry Research Institute Liaison Council (2008). Changes in the distributions of pine wilt disease and the vector beetle *Monochamus alternatus* in the Tohoku region of northern Japan. *Bulletin of the Forestry and Forest Products Research Institute*, 7, 139–158.
- Forest Conservation Departmental Meeting of Tohoku Forestry Research Institute Liaison Council (2014). Changes in the distributions of pine wilt disease and the vector beetle *Monochamus alternatus* in the Tohoku region of northern Japan between 2007 and 2011. *Bulletin of the Forestry and Forest Products Research Institute*, 13, 335–343.
- Hanski, I., & Thomas, C. D. (1994). Metapopulation dynamics and conservation - a spatially explicit model applied to butterflies. *Biological Conservation*, 68, 167–180. [https://doi.org/10.1016/0006-3207\(94\)90348-4](https://doi.org/10.1016/0006-3207(94)90348-4)
- Hastings, A., Cuddington, K., Davies, K. F., Dugaw, C. J., Elmendorf, S., Freestone, A., ... Thomson, D. (2005). The spatial spread of invasions: New developments in theory and evidence. *Ecology Letters*, 8, 91–101. <https://doi.org/10.1111/j.1461-0248.2004.00687.x>
- Igarashi, M. (1977). Biology of *Monochamus alternatus* in Tohoku (II): Larval development in natural condition. *Annual Report of the Tohoku Branch, Forest Experiment Station*, 18, 128–133.
- Ishigooka, Y., Kuwagata, T., Nishimori, M., Hasegawa, T., & Ohno, H. (2011). Spatial characterization of recent hot summers in Japan with agro-climatic indices related to rice production. *Journal of Agricultural Meteorology*, 67, 209–224. <https://doi.org/10.2480/agrmet.67.4.5>
- Jikumaru, S., & Togashi, K. (2000). Temperature effects on the transmission of *Bursaphelenchus xylophilus* (Nemata: Aphelenchoididae) by *Monochamus alternatus* (Coleoptera: Cerambycidae). *Journal of Nematology*, 32, 110–116.
- Johnson, D. M., Liebhold, A. M., Tobin, P. C., & Bjørnstad, O. N. (2006). Allee effects and pulsed invasion by the gypsy moth. *Nature*, 444, 361–363. <https://doi.org/10.1038/nature05242>
- Kawai, M., Shoda-Kagaya, E., Maehara, T., Zhou, Z., Lian, C., Iwata, R., ... Hogetsu, T. (2006). Genetic structure of pine sawyer *Monochamus alternatus* (Coleoptera: Cerambycidae) populations in northeast Asia: Consequences of the spread of pine wilt disease. *Environmental Entomology*, 35, 569–579. <https://doi.org/10.1603/0046-225X-35.2.569>
- Keitt, T., Lewis, M. A., & Holt, R. D. (2001). Allee effects, invasion pinning, and species' borders. *The American Naturalist*, 157, 203–216. <https://doi.org/10.1086/318633>
- Kishi, Y. (1995). *The pine wood nematode and the Japanese pine sawyer*. Tokyo, Japan: Thomas Company Limited.
- Lewis, M. A., & Kareiva, P. (1993). Allee dynamics and the spread of invading organisms. *Theoretical Population Biology*, 43, 141–158. <https://doi.org/10.1006/tpbi.1993.1007>
- MacKenzie, D. I., Nichols, J. D., Hines, J. E., Knutson, M. G., & Franklin, A. B. (2003). Estimating site occupancy, colonization, and local extinction probabilities when a species is detected imperfectly. *Ecology*, 84, 2200–2207. <https://doi.org/10.1890/02-3090>
- MacKenzie, D. I., Nichols, J. D., Seamans, M. E., & Gutiérrez, R. J. (2009). Modeling species occurrence dynamics with multiple states and imperfect detection. *Ecology*, 90, 823–835. <https://doi.org/10.1890/08-0141.1>
- Mamiya, Y. (1988). History of pine wilt disease in Japan. *Journal of Nematology*, 20, 219–226.
- Mota, M. M., Futai, K., & Vieira, P. (2009). Pine wilt disease and the pinewood nematode, *Bursaphelenchus xylophilus*. In A. Ciancio, & K. G. Mukerji (Eds.), *Integrated management of fruit crops nematodes* (pp. 253–274). Dordrecht, the Netherlands: Springer. <https://doi.org/10.1007/978-1-4020-9858-1>
- Nakamura, K. (2008). Attraction trap for monitoring *Monochamus alternatus* adults - its usefulness and limitations. In M. M. Mota, & P. Vieira (Eds.), *Pine wilt disease: A worldwide threat to forest ecosystems* (pp. 369–378). Dordrecht, the Netherlands: Springer.
- Nakazawa, T., Yamanaka, T., & Urano, S. (2012). Model analysis for plant disease dynamics co-mediated by herbivory and herbivore-borne phytopathogen. *Biology Letters*, 8, 685–688. <https://doi.org/10.1098/rsbl.2012.0049>
- Osada, Y., Yamakita, T., Shoda-Kagaya, E., Liebhold, A. M., & Yamanaka, T. (2018). Data from: Disentangling the drivers of invasion spread in a vector-borne tree disease. *Dryad Digital Repository*, <https://doi.org/10.5061/dryad.61c4h39>
- Ovaskainen, O., & Hanski, I. (2001). Spatially structured metapopulation models: Global and local assessment of metapopulation capacity. *Theoretical Population Biology*, 60, 281–302. <https://doi.org/10.1006/tpbi.2001.1548>
- Plummer, M. (2003). JAGS: A program for analysis of bayesian graphical models using gibbs sampling. *Proceedings of the 3rd International Workshop on Distributed Statistical Computing (DSC 2003)*. March, pp. 20–22.
- R Core Team (2017). *R: A Language and Environment for Statistical Computing*. R Development Core Team, Vienna, Austria.
- Robinet, C., Opstal, N. V., Baker, R., & Roques, A. (2011). Applying a spread model to identify the entry points from which the pine wood nematode, the vector of pine wilt disease, would spread most rapidly across Europe. *Biological Invasions*, 13, 2981–2995. <https://doi.org/10.1007/s10530-011-9983-0>
- Royle, J. A., & Nichols, J. D. (2003). Estimating abundance from repeated presence-absence data or point counts. *Ecology*, 84, 777–790. [https://doi.org/10.1890/0012-9658\(2003\)084\[0777:EAFRPA\]2.0.CO;2](https://doi.org/10.1890/0012-9658(2003)084[0777:EAFRPA]2.0.CO;2)
- Sata, I. (1942). *Pine boring insects and protection in Hyogo*. (In Japanese) Hyogo prefectural forestry study station. 53 pp.
- Seino, H. (1993). An estimation of distribution of meteorological elements using GIS and AMeDAS data. *Journal of Agricultural Meteorology*, 48, 379–383. <https://doi.org/10.2480/agrmet.48.379>
- Shin, S.-C. (2008). Pine wilt Disease in Korea. In B. G. Zhao, K. Futai, J. R. Sutherland, & Y. Takeuchi (Eds.), *Pine wilt disease* (pp. 26–32). Netherlands: Springer. <https://doi.org/10.1007/978-4-431-75655-2>
- Stout, M. J., Thaler, J. S., & Thomma, B. P. H. J. (2006). Plant-mediated interactions between pathogenic microorganisms and herbivorous arthropods. *Annual Review of Entomology*, 51, 663–689. <https://doi.org/10.1146/annurev.ento.51.110104.151117>
- Takasu, F., Yamamoto, N., Kawasaki, K., Togashi, K., Kishi, Y., & Shigesada, N. (2000). Modeling the expansion of an introduced tree disease. *Biological Invasions*, 2, 141–150. <https://doi.org/10.1023/A:1010048725497>
- Taketani, A., Okuda, M., & Hosoda, R. (1975). The meteorological analysis on the epidemic mortality of pine trees, with special reference to the effective accumulated temperature. *Journal of the Japanese Forestry Society*, 57, 169–175. https://doi.org/10.11519/jjfs1953.57.6_169
- Taylor, C. M., & Hastings, A. (2004). Finding optimal control strategies for invasive species: A density-structured model for *Spartina alterniflora*. *Journal of Applied Ecology*, 41, 1049–1057. <https://doi.org/10.1111/j.0021-8901.2004.00979.x>
- Tisseuil, C., Gryspeirt, A., Lancelot, R., Pioz, M., Liebhold, A., & Gilbert, M. (2016). Evaluating methods to quantify spatial variation in the velocity of biological invasions. *Ecography*, 39, 409–418. <https://doi.org/10.1111/ecog.01393>
- Tobin, P. C., Whitmore, S. L., Johnson, D. M., Bjørnstad, O. N., & Liebhold, A. M. (2007). Invasion speed is affected by geographical variation in the strength of Allee effects. *Ecology Letters*, 10, 36–43. <https://doi.org/10.1111/j.1461-0248.2006.00991.x>
- Togashi, K. (2008). Vector-nematode relationships and epidemiology in pine wilt disease. In B. G. Zhao, K. Futai, J. R. Sutherland, & Y.

- Takeuchi (Eds.), *Pine wilt disease* (pp. 162–183). Dordrecht, the Netherlands: Springer. <https://doi.org/10.1007/978-4-431-75655-2>
- Togashi, K., & Shigesada, N. (2006). Spread of the pinewood nematode vectored by the Japanese pine sawyer: Modeling and analytical approaches. *Population Ecology*, *48*, 271–283. <https://doi.org/10.1007/s10144-006-0011-7>
- Turchin, P., & Thoeny, W. (1993). Quantifying dispersal of southern pine beetles with mark-recapture experiments and a diffusion model. *Ecological Applications*, *3*, 187–198. <https://doi.org/10.2307/1941801>
- Veran, S., Simpson, S. J., Sword, G. A., Deveson, E., Piry, S., Hines, J. E., & Berthier, K. (2015). Modeling spatiotemporal dynamics of outbreaking species: Influence of environment and migration in a locust. *Ecology*, *96*, 737–748. <https://doi.org/10.1890/14-0183.1>
- Watanabe, J., Togashi, M., & Arai, T. (1987). Study on the disaster prevention forests in coastal area (*Kaigan-Bousairin ni Kansuru Kenkyu*). *Bulletin of the Fukushima Prefectural Forest Experiment Station*, *20*, 105–122. (in Japanese).
- Yamanaka, T., & Liebhold, A. M. (2009). Spatially implicit approaches to understand the manipulation of mating success for insect invasion management. *Population Ecology*, *51*, 427–444. <https://doi.org/10.1007/s10144-009-0155-3>
- Yamanaka, T., Nelson, W. A., Uchimura, K., & Bjørnstad, O. N. (2012). Generation separation in simple structured life-cycles: Models and 48 years of field data on a tea tortrix moth. *The American Naturalist*, *179*, 95–109. <https://doi.org/10.1086/663201>
- Yoshida, N. (2006). A strategy for controlling pine wilt disease and its application on-site. *Journal of Japanese Forest Society*, *88*, 422–428. <https://doi.org/10.4005/jjfs.88.422>
- Yoshimura, A., Kawasaki, K., Takasu, F., Togashi, K., Futai, K., & Shigesada, N. (1999). Modeling the spread of pine wilt disease caused by nematodes with pine sawyers as vector. *Ecology*, *80*, 1691–1702. [https://doi.org/10.1890/0012-9658\(1999\)080\[1691:MTSOPW\]2.0.CO;2](https://doi.org/10.1890/0012-9658(1999)080[1691:MTSOPW]2.0.CO;2)
- Zhao, B. G. (2008). Pine wilt disease in China. In B. G. Zhao, K. Futai, J. R. Sutherland, & Y. Takeuchi (Eds.), *Pine wilt disease* (pp. 18–25). Dordrecht, the Netherlands: Springer. <https://doi.org/10.1007/978-4-431-75655-2>

SUPPORTING INFORMATION

Additional supporting information may be found online in the Supporting Information section at the end of the article.

How to cite this article: Osada Y, Yamakita T, Shoda-Kagaya E, Liebhold AM, Yamanaka T. Disentangling the drivers of invasion spread in a vector-borne tree disease. *J Anim Ecol*. 2018;87:1512–1524. <https://doi.org/10.1111/1365-2656.12884>